JOURNAL OF NANO- AND ELECTRONIC PHYSICS
Vol. **6** No 4, 04020(5pp) (2014)

ЖУРНАЛ НАНО- ТА ЕЛЕКТРОННОЇ ФІЗИКИ
Том **6** № 4, 04020(5cc) (2014)

Topological Features of the Vapor-Phase SnTe Nanostructures on Polyamide

Ya.P. Saliy[1], I.I. Chaviak[2], I.S. Bylina[1,*], D.M. Freik[1]

[1] *Vasyl Stefanyk PreCarpathian National University 57, Shevchenko Str., 76018 Ivano-Frankivsk, Ukraine*
[2] *Ivano-Frankivsk National Medical University, 2, Halyzka Str., 76000 Ivano-Frankivsk, Ukraine*

(Received 05 August 2014; published online 29 November 2014)

The results of the study of nanostructures on the surface of tin telluride thin films deposited from the vapor phase on polyamide substrates by open evaporation in vacuum are presented. Computer analysis of the results of the atomic force microscopy has revealed the influence of the technological factors on the shape features and surface orientation of nanoislands. It is shown that nanostructures of various sizes are dome-shaped with a small ratio of height to lateral diameter. A weak dependence of the island symmetry on the technological factors of deposition is found.

Keywords: Tin telluride, Nanostructures, Vapor-phase technology, Atomic force microscopy, Growth processes.

PACS numbers: 64.60.Gj, 68.03.Fg

1. INTRODUCTION

Currently, the efforts of scientists are intended for the development of new materials using nanotechnologies [1, 2]. The latter imposes requirements on the analytical methods of investigation of nanostructures and nanoobjects which should allow obtaining the reliable quantitative characteristics. Atomic force microscopy (AFM), high resolution electron microscopy open up new possibilities of observation and analysis of the growth stages of different nanoobjects.

Using nanotechnologies at deposition of lead and tin tellurides, they fabricate quantum-size structures with specified electron spectrum and necessary optical, electrical and other properties [1, 2]. It is possible to produce on their basis heterolasers and light emitting diodes from the near IR to blue light range, infrared photodetectors and thermoelectric heat energy converters for the medium temperature range (500-850 K) [3, 4]. Thus, in particular, the authors of [2] have reported that ensemble of quantum dots is created in PbSe/PbTe heterosystem, and the authors of [5] have described the chemical synthesis of SnTe nanocrystals using triethanol as a stabilizing element. X-ray diffraction and selective surface diffraction of electrons have shown that nanoparticles had the rock salt cubic structure and band gap could be shifted toward the blue region of the optical spectrum by changing the nanocrystal size.

Self-organization processes often underlie the formation of nanostructures by the deposition method. However, for the detailed study of the growth stages it is necessary to decrease rate and time of material deposition on the substrate that is possible in the vapor-phase methods. In this case, one can control the island sizes by changing the growth conditions.

In the work, vapor-phase SnTe deposition processes on polyamides are investigated based on the analysis of the AFM images and periodicity and symmetry of cluster arrangement on the structure surface are established as well as the influence of deposition temperature and time.

2. MATERIALS AND METHODS OF INVESTIGATION

Vapor-phase condensates were obtained by the evaporation of synthesized SnTe compound in the open vacuum with subsequent deposition on a polyamide substrate of the PM-1 type. Before vapor deposition, the substrate was thermally annealed at the temperature of 140 °C for 30 minutes. Substrate temperature during the growth was varied in the range of T_{Sub} = 140-200 °C and growth time τ was equal to 2-30 min. Shutdown of the deposition process was performed using a shutter which was located between the source and substrate.

For the investigation of the surface morphology of SnTe layers we have applied the AFM method Nanoscope 3a Dimension 3000 (Digital Instruments USA) in the periodic contact mode. Measurements were carried out in the central part of the samples using series silicon probes NSG-11 with the nominal bending radius of the point to 10 nm (NT0MDT, Russia). Based on the results of the AFM investigations, sizes of nanocrystals in the lateral direction and height increments are defined in Excel besides the surface morphology and profilograms. For the analysis of the morphological features of nanostructures on the surface of deposited SnTe films using Gwyddion software we have determined the polar ρ and azimuth φ angles for all points of the surfaces as well as for faces of separate nanocrystals according to which angles θ between the normals to them were calculated.

The obtained experimental results were analyzed by using the discrete Fourier transformation $F(k)$ of function $f(n)$ according to

$$F(k) = \Sigma f(n)\exp(-i\, n\, 2\, \pi\, k / N) \qquad (1)$$

and autocorrelation function $C(l)$ of the distribution of the azimuth angle φ of nano-objects, respectively,

$$C(l) = (\Sigma f(l + n) f(n) / N)^{1/2}. \qquad (2)$$

Here k is the harmonic index of the distribution function; n is the number of the experimental value of angle φ; N is the amount of values of angle φ; l is the shift step of the distribution function.

* vanjabylina@gmail.com

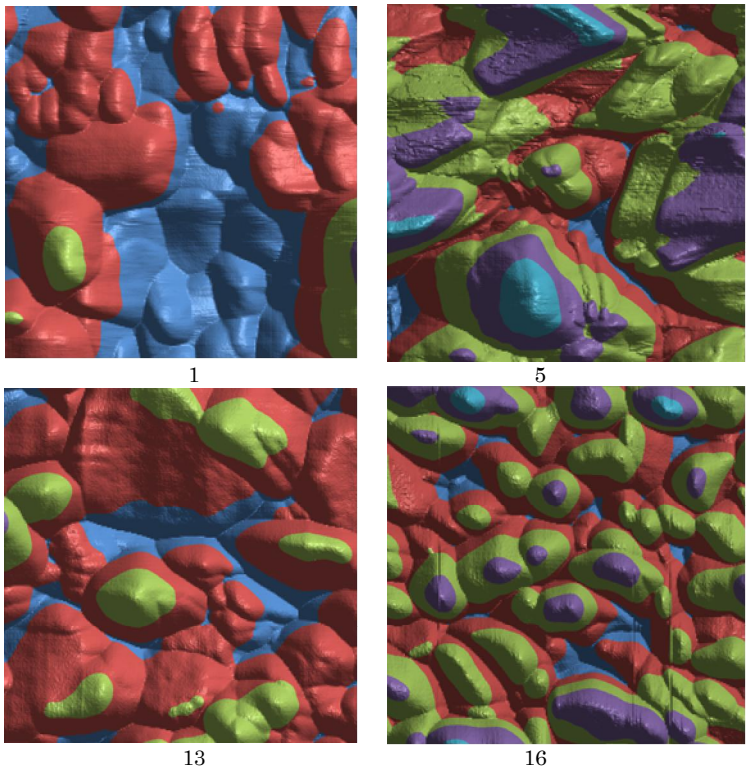

Fig. 1 – AFM-topograms of the surface of SnTe films on polyamide. Integers correspond to the sample numbers from Table 1

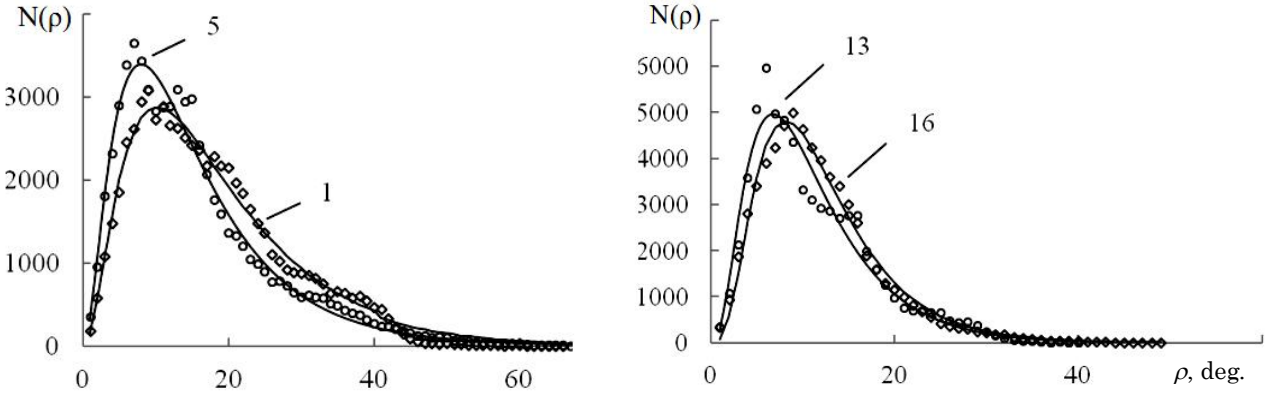

Fig. 2 – Distribution of the polar angle $N(\rho)$ for nanostructures on the SnTe/polyamide film surface. Integers near the dependences correspond to the sample numbers from Table 1

Table 1 – Technological parameters of the deposition of SnTe films on polyamide

Sample	Evaporator temperature T_E, °C	Substrate temperature T_{Sub}, °C	Deposition time τ, minutes
1	590	140	10
5	590	140	28
13	650	200	4
16	650	200	19

Table 2 – Approximation coefficients of the distribution of the polar angles ρ by the function (3) for nanostructures in SnTe/polyamide films

Sample	N_{max}	a	λ	β
1	720	2.94	1.56	0.539
5	1700	2.84	1.69	0.543
13	3600	3.93	2.54	0.545
16	1900	5.26	3.40	0.520

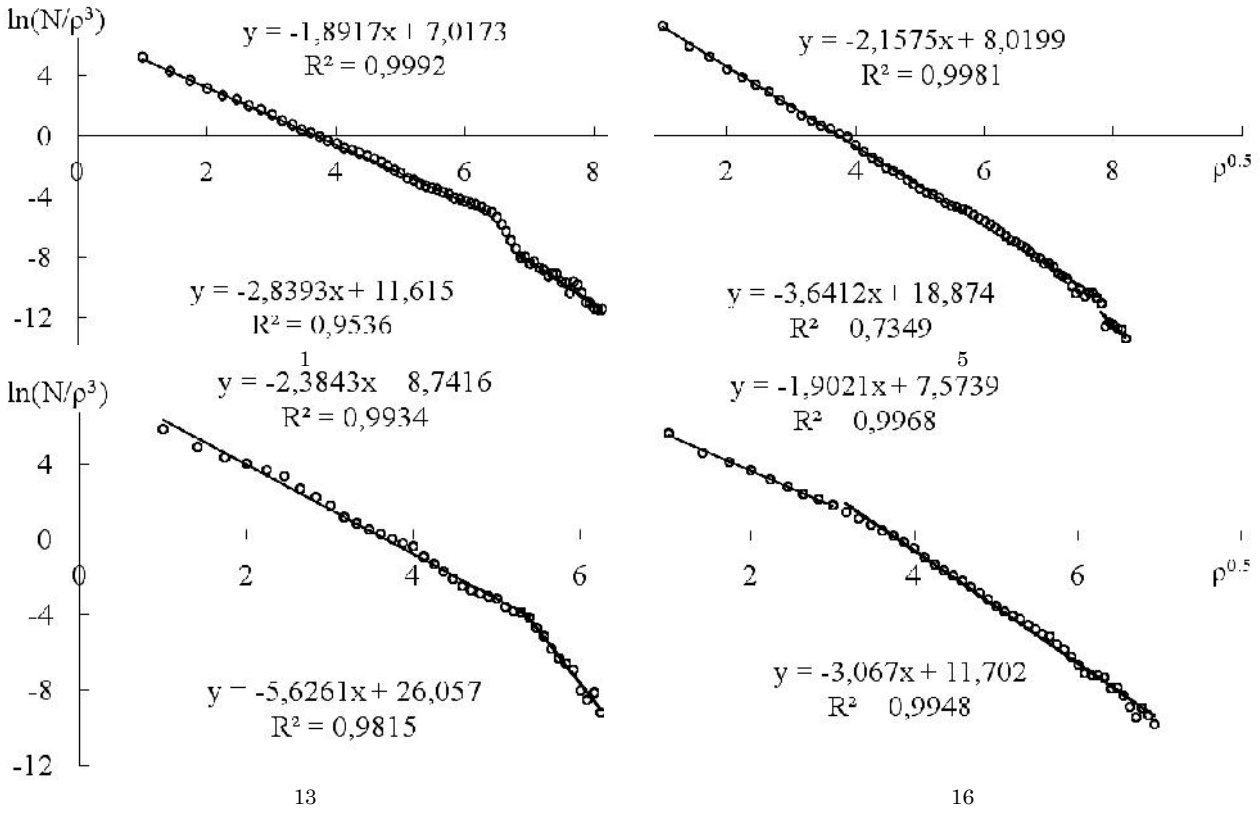

Fig. 3 – Curves and functions ($y = ln(N / p^3)$, $x = \rho^{0.5}$) and also the values of the determination coefficient R^2 of the linearized distribution of the polar angle ρ for nanostructures on the SnTe/polyamide film surface. Integers near the curves correspond to the sample numbers from Table 1

Layer thickness was determined by the measurement of the step height obtained by the removal of SnTe layer from a part of the surface of each sample.

3. EXPERIMENTAL RESULTS AND DISCUSSION

As the results of the AFM investigations of condensates showed, an array of three-dimensional islands is formed on the surface of SnTe/polyamide structures (see Fig. 1). The island shape is dome-like and resembles the shape of "dome clusters" of germanium on silicon [6]. In this case, a spread of islands in values is observed. The average altitude difference on the samples 1, 5, 13, 16 (Table 1) is equal to 100, 60, 40, 30 nm and the average lateral size of pyramidal and wedge-like objects is 250, 500, 300, 100 nm, respectively. Height-to-lateral section ratio for these objects is approximately 0.4, 0.1, 0.1, 0.3. As seen, nanostructures on the surface are merged and their concentration decreases by 2 times from 10^9 cm^{-2} to 5 10^8 cm^{-2} with increasing deposition time τ from 10 to 28 min at the substrate temperature T_{Sub} = 140 °C. Otherwise, nano-objects on the film surfaces grown at the temperature of T_{Sub} = 200 °C are isolated with the change in the deposition time from 4 to 19 min and their concentration increases by 5 times from 10^9 cm^{-2} to 5 10^9 cm^{-2}.

3.1 Polar angle distribution

Polar angle ρ distribution along the normal to the film surface scanned by the microscope should confirm or refute the thesis about pyramidal shape of the objects on the film surface. This distribution should be narrow in the vicinity of a certain angle which corresponds to the slope of nanocrystal faces to the horizontal film surface. In Fig. 2 we illustrate the histograms of the polar angle ρ distribution which show the number of values N of angle ρ hitting into the range $\Delta\rho = 1°$. It is seen that the change in the deposition time τ and substrate temperature T_{Sub} does not considerably influence the position of the distribution maxima which is in the vicinity of 10°. Increase in the deposition temperature T_{Sub} from 140 to 200 °C narrows this distribution by ~ 2 times. Thus, islands have a plane shape that was already indicated by their height-to-lateral diameter ratios.

Polar angle distributions were approximated by a smooth function of the form

$$N(\rho) = N_{\max}\, \rho^{\alpha} \exp(-\lambda\rho^{\beta}). \qquad (3)$$

Here $N_{\max}$, α, λ, β are the approximation coefficients.

In Table 2 we present the values of these approximation coefficients. It is seen (Table 2) that coefficient β for all dependences is almost the same and equal to $\beta \approx 0.5$. For the first couple of samples 1 and 5 (Table 2) coefficients α and λ are also approximately equal ($\alpha \approx 3$, $\lambda \approx 1.6$). Based on this, there is a possibility of linearization of the experimental curves in $ln(N/\rho^3) - \rho^{0.5}$ coordinates

$$\ln(N / \rho^3) = \ln(N_{max}) - \lambda\rho^{0.5}. \qquad (4)$$

In Fig. 3 we illustrate dependences (4) for the investigated samples. Experimental results in these coordinates are approximated by two straight lines which can

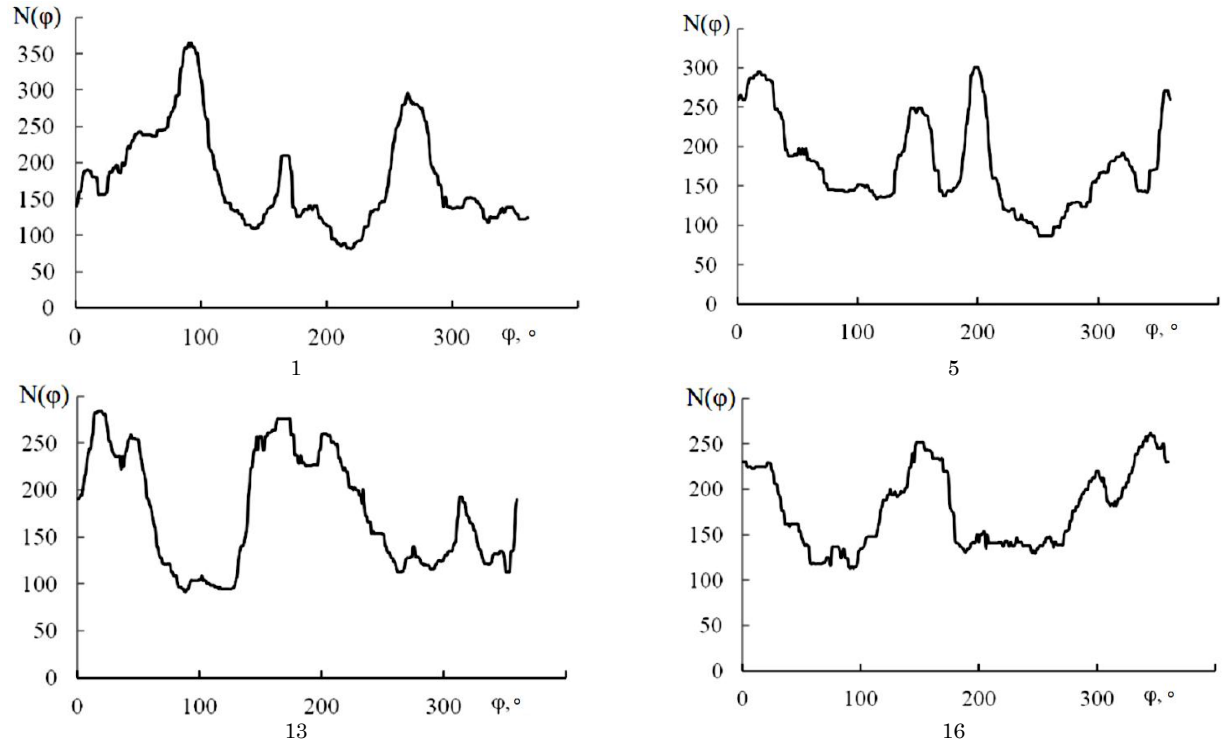

Fig. 4 – Azimuth angle distribution $N(\varphi)$ for nanostructures on the SnTe/polyamide film surface. Integers below the graphs correspond to the sample numbers from Table 1

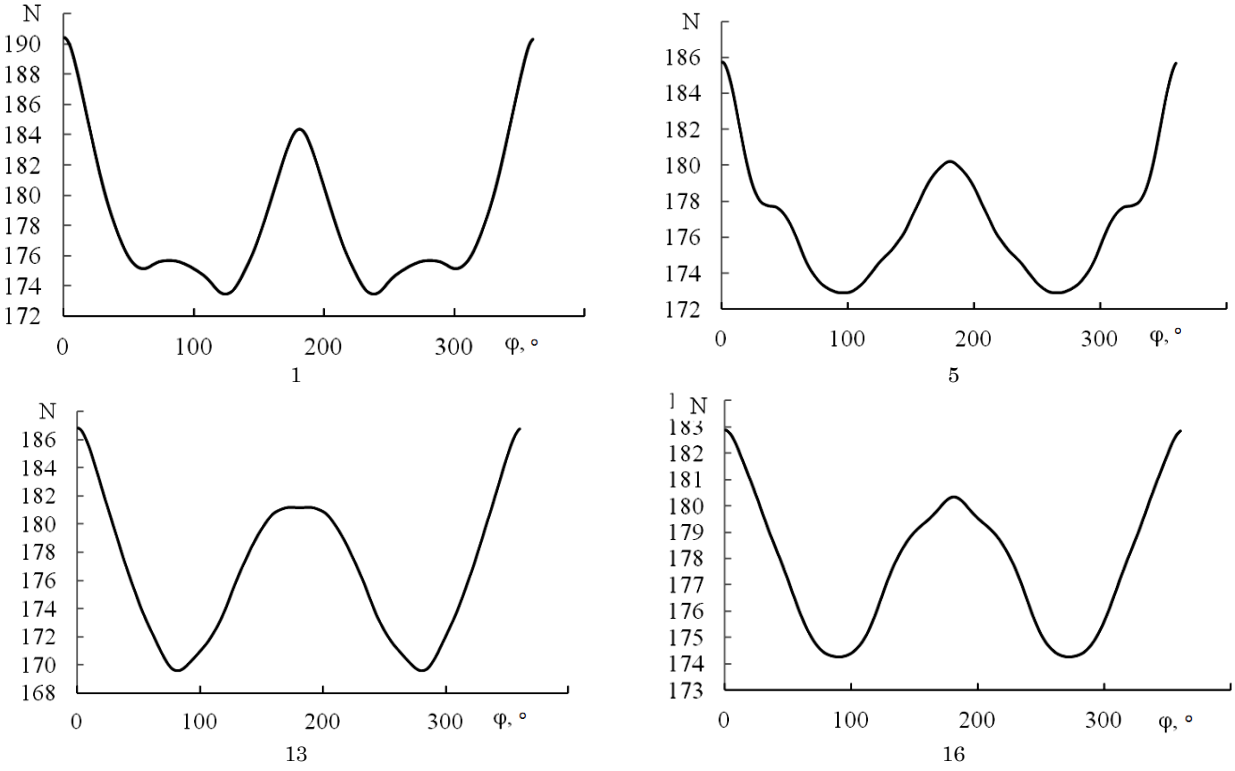

Fig. 5 – Autocorrelation function of the azimuth angle φ for nanostructures on the SnTe/polyamide film surface. Integers below the graphs correspond to the sample numbers from Table 1

be responsible for different processes of the nano-object formation on the condensate surface: plane and formed pyramidal structures (Fig. 1). It was revealed here that cross point of the approximated straight lines and the abscissa axis for all samples is equal to ~ 3.71 that corresponds to the angle $\rho = 14°$.

3.2 Azimuth angle distribution

Now we consider anisotropy evolution of the surface objects depending on the temperature regime and deposition time. Azimuth angle φ represents the direction of the orientation of lateral surfaces of nanostructures in the substrate plane. Azimuth angles distributions and autocorrelation functions of these distributions, which correspond to the samples 1, 5, 13, 16, are illustrated in Fig. 4 and Fig. 5, respectively. The first (1, 5) and the second (13, 16) couples of samples are obtained under different temperature conditions, and deposition time inside each couple increases with the sample number. We observe four different autocorrelation functions with the maximum for angle ~ 180° that corresponds to the presence of the second-order symmetry axis in objects (see Fig. 5). In the first couple obtained at the substrate temperature T_{Sub} = 140 °C and evaporator temperature T_E = 590 °C (sample 1 with lesser deposition time τ = = 10 min, see Table 1) there is an additional peak near φ = 90° that implies the presence of the four-order axis. With increasing deposition time to τ = 28 min (sample 5, Table 1) this additional peak disappears but peaks at φ = 45° and φ = 120° appear (Fig. 4 – 5). The last angle value indicates the third-order axis. For the second couple of samples (T_{Sub} = 200 °C, T_E = 650 °C) increase in the evaporator temperature by 60 °C led to the extension of the peak at φ = 180° (Fig. 4 – 13, 16). Increase in the deposition time from 4 min (sample 13, Table 1) to 19 min (sample 16, Table 1) influenced to appearance of the peak at 140° that implies the formation on the condensate surface of pentagon dodecahedrons (Fig. 5 – 16).

3.3 Angles between faces

Analysis of the angles between normals to four faces of separate nano-objects for the sample 1 (Table 1) is equal to 60° that corresponds to the faces of the system {110} of rhombic dodecahedron. Fourier transformation of the azimuth angle φ distribution gives the prevalence of the four-order axis over the higher order axes by 3 times. Angles between three faces of some nano-objects of the sample 5 (Table 1) are equal to 45°, 45°, 60°. This means that crystal planes of the system {100} of cube are additionally manifested. Prevalence of the four-order axis over the third-order axis remains based on the Fourier transformation, but the five-, six-, seven-, eight-order axes become comparable with the four-order axis. This is exhibited on the automodal function by the peak at ~ 45° (Fig. 5 – 5). For the samples 13, 16 (Table 1) one observe the prevalence of the third-order axis by the Fourier transformation and this corresponds to the angle of 120° (Fig. 5 – 13, 16) on the auto-modal function.

Nano-objects on the surface of SnTe condensates can correspond by dihedral angles θ to the hexaoctahedron with the faces {123}. In particular, angle between the faces (123) and (132) is equal to θ = 21.8° that is observed experimentally.

4. CONCLUSIONS

1. The crystallographic analysis of separate nanoformations has been performed based on the AFM-images of the vapor-phase SnTe/polyamide condensate surfaces.

2. Formation conditions of plane and pyramidal nano-objects with the change in the vapor deposition time at different substrate temperatures have been established by the linearized approximation of the polar angle distribution.

3. Using the Fourier transformation and autocorrelation function of the distribution of azimuth angles of nanocrystallites it is shown that complex crystallographic forms, which correspond to the planes {100} and {110} of cube and rhombic dodecahedron and also to the planes {123} of hexaoctahedron, are realized in the vapor-phase SnTe/polyamide condensates.

AKNOWLEDGEMENTS

This work has been performed in the framework of the scientific project of the National Academy of Sciences of Ukraine (Project No 0110U006281).

REFERENCES

1. D.M. Freik, M.A. Galushchak, L.I. Mezhylovskaya, *Fizika i tekhnologiya poluprovodnikovyh plenok* (Lviv: Vyshcha shkola: 1988).
2. S.P. Zimin, E.S. Gorlachev, *Nanostrukturirovannye khalkogenidy svintsa* (Yaroslavl': YarGU: 2011).
3. A.N. Mikhaylov, A.I. Belov, A.B. Kostyuk, *Phys. Solid State* **57**, 368 (2012).
4. K. Alchalabi, D. Zimin. G. Kostorz, H. Zogg, *Phys. Rev. Lett.* **90**, 026104 (2003).
5. Ying Xu, Najeh Al-Salim, Justin M. Hodgkiss, Richard D. Tilley, *Cryst. Growth Des.* **11** No7, 2721 (2011).
6. G. Medeiros-Ribeiro, A.M. Bratkovski, T.I. Kamins, A.A. Ohlberg, R.S. Williams, *Science* **279**, 353 (1998).